The 26Mg(3He,n)28Si Reaction at 23.1 and 45.5 MeV

I. 4 The $^{26}Mg(^{3}He,n)^{28}Si$ Reaction at 23.1 and 45.5 MeV

Abe K., Ishimatsu T.*, Kawamura T.*, Maeda K., Furukawa T.*, Orihara H.** and Zafiratos C. D.***
College of General Education, Tohoku University
Department of Physics, Faculty of Science, Tohoku University*
Cyclotron and Radioisotope Center, Tohoku University**
University of Colorado, USA***

We have made an experiment of the $^{26}Mg(^{3}He,n)^{28}Si$ reaction, and analyzed the experimental data within the framework of zero-range DWBA using theoretical two-nucleon spectroscopic amplitudes.[1] The results were reported partly in a previous issue of the CYRIC Annual Report.[2] These calculations failed in some cases in reproducing the experimental data, and we tried to make a further analysis of the data by taking account of two-step processes. We present here the results of this analysis.

We made coupled-channel as well as DWBA calculations for the $^{26}Mg(^{3}He,n)^{28}Si$ reactions leading to the lowest four states in ^{28}Si. The two-step transitions taken into account in the coupled-channel calculations are shown in figs. 1 and 2. The present calculations were performed with the code CHUCK.[3] The optical-model parameters were taken from the global potentials; the B2 set of Becchetti et al.[4] for ^{3}He parameters, the "best fit" set of Becchetti and Greenlees[5] for neutron parameters, and the set L of Daehnick et al.[6] for deuteron parameters. The Bayman-Kallio[7] form factor was used for the direct two-nucleon transfer. The bound-state parameters were r_0=1.25 fm, a=0.65 fm and λ=25. Whenever we make coupled-channel calculations like the present ones, we must have a reliable value of the normalization constant or enhancement factor ε for the direct $(^{3}He,n)$ transitions, which is not yet well established. We found that the neutron angular distributions for the $^{26}Mg(^{3}He,n)^{28}Si$ ground-state reaction observed at bombarding energies of 23.1 and 45.5 MeV were reproduced as described below by coupled-channel calculation when an enhancement factor ε=1.4 was used together with a zero range strength $D_0^2=25\times10^4$ $MeV^2\cdot fm^3$, and we used these values of ε and D_0^2 throughout the present analysis.

In the present calculations we used the shell-model two-nucleon spectroscopic amplitudes[1] to obtain the coupling strengths between initial and final channels. The coupling strengths between initial and intermediate channels and those between final and intermediate channels were obtained from the spectroscopic factors C^2S and deformation parameter β_2 listed in table 1, where all but C^2S for the transitions (3)→(5) and (6)→(7) are experimental. We see in table 1 that the intermediate channels we took account of are empirically known to have comparatively strong couplings with the initial

and/or the final channels, and the two-step transitions via them may have important contributions to the observed cross sections. Phases or signes of the spectroscopic amplitudes needed for coupled-channel calculation cannot be determined from C^2S and β_2. We found that the phase combinations of spectroscopic amplitudes listed in table 2 were the only ones that reproduced the observed neutron angular distributions in shape as well as in magnitude. As an example, fig. 3 shows the results of the coupled-channel calculations for the $^{26}Mg(^3He,n)^{28}Si$ reaction leading to the 4.62-MeV 4^+ state at 45.5 MeV bombarding energy made by using four different phase combinations of spectroscopic amplitudes. Of these four calculated curves, only the thick solid curve reproduced successfully the experimental data as shown in fig. 5.

Figs. 4 and 5 show the experimental neutron angular distributions for the $^{26}Mg(^3He,n)^{28}Si$ reactions leading to the lowest four states measured respectively at 23.1 and 45.5 MeV bombarding energies. Since the neutron groups corresponding to the 4.62-MeV 4^+ second-excited and the 4.98-MeV 0^+ third-excited states were not separated in the present experiment, the composite angular distributions of these two groups were measured and are shown in figs. 4 and 5. The solid curves are the results of the coupled-channel calculations, and the broken curves are those of the DWBA calculations; these curves are to be compared with the experimental data. The thin broken curves (a) are the results of the coupled-channel calculations for the 4.62-MeV 4^+ state, and the dotted curves (b) are those for the 4.98-MeV 0^+ state.

We see in figs. 4 and 5 that all the experimental angular distributions are reproduced fairly well both in shape and in magnitude by the coupled-channel calculations. In most of the cases the experimental data are reproduced by the DWBA calculations as well, which indicates seemingly that the contributions of two-step processes are unimportant. It should be noted, however, that the experimental data of the 1.78 MeV state at 45.5 MeV bombarding energy and those of the unresolved 4.62 and 4.98 MeV states at 23.1 MeV bombarding energy are reproduced satisfactorily when the two-step transitions are taken into account. This suggests that when analyzing experimental data of the $(^3He,n)$ reaction we have to take account of two-step processes properly, or we may be led in some cases to wrong conclusions.

References

1) Bohne W., Büchs K. D., Fuchs H., Grabisch K., Hilscher D., Jahnke U., Kluge H., Masterson T. G., Morgenstern H. and Wildenthal B. H., Nucl. Phys. A378 (1982) 525.
2) Abe K., Kawamura T., Maeda K., Ishimatsu T., Furukawa K., Orihara H. and Zafiratos C. D., CYRIC Ann. Rep. 1983, p. 10.
3) Kunz P. D., private communication.
4) Becchetti F. D., Makofske W. and Greenlees G. W., Nucl. Phys. A190 (1972) 437.

5) Becchetti F. D. and Greenlees G. W., Phys. Rev. 182 (1969) 1190.
6) Daehnick W. W., Childs J. D. and Vrcelj Z., Phys. Rev. C21 (1980) 2253.
7) Bayman B. F. and Kallio A., Phys. Rev. 156 (1967) 1121.
8) Luts H. F., Heikkinen D. W., Bartolini W. and Curtis T. H., Phys. Rev. C2 (1970) 981.
9) Barnard R. W. and Jones G. D., Nucl. Phys. A108 (1968) 641.
10) Mackh H., Mairle G. and Wagner G. J., Z. Phys. 269 (1974) 353.
11) Barnard R. W. and Jones G. D., Nucl. Phys. A108 (1968) 655.

Table 1. Spectroscopic factors and deformation parameter used in the coupled-channel calculations.

Transition[a]	ℓ	$n\ell_j$[b]	C^2S	β_2
(1)→(2)	2	$1d_{5/2}$	0.25[c]	
(1)→(3)	0	$2s_{1/2}$	0.50[c]	
(1)→(6)	2	$1d_{3/2}$	0.61[c]	
(2)→(4)	2	$1d_{5/2}$	2.64[d]	
(2)→(5)	0	$2s_{1/2}$	0.46[d]	
(2)→(7)	2	$1d_{3/2}$	0.21[d]	
(2)→(8)	2	$1d_{5/2}$	0.30[d]	
(3)→(4)	0	$2s_{1/2}$	0.79[e]	
(3)→(5)	2	$1d_{5/2}$	0.25[f]	
(4)→(5)				0.57[g]
(6)→(7)	2	$1d_{5/2}$	0.25[h]	

[a] See figs. 1 and 2.
[b] Bound state of transferred particle.
[c] Ref. 8). [d] Ref. 9). [e] Ref. 10).
[f] Theoretical value for the transition between the configurations $[(d_{5/2})^{10}_{0,1}(s_{1/2})^{1}_{1/2,1/2}]_{1/2,1/2}$ and $[(d_{5/2})^{11}_{5/2,1/2}(s_{1/2})^{1}_{1/2,1/2}]_{2,0}$.
[g] Ref. 11).
[h] Theoretical value for the transition between the configurations $[(d_{5/2})^{10}_{0,1}(d_{3/2})^{1}_{3/2,1/2}]_{3/2,1/2}$ and $[(d_{5/2})^{11}_{5/2,1/2}(d_{3/2})^{1}_{3/2,1/2}]_{4,0}$.

Table 2. Sign of the product of two spectroscopic amplitudes of individual steps in a two-step transition.

Two-step transition[a]	Sign[b]
(1) → (2) → (4)	-
(1) → (3) → (4)	+
(1) → (2) → (5)	+
(1) → (3) → (5)	-
(1) → (4) → (5)	+
(1) → (2) → (7)	-
(1) → (6) → (7)	-
(1) → (2) → (8)	-

[a] See figs. 1 and 2.

[b] The shell-model two-nucleon spectroscopic amplitudes given in ref. 1) are used for the direct two-proton stripping transitions.

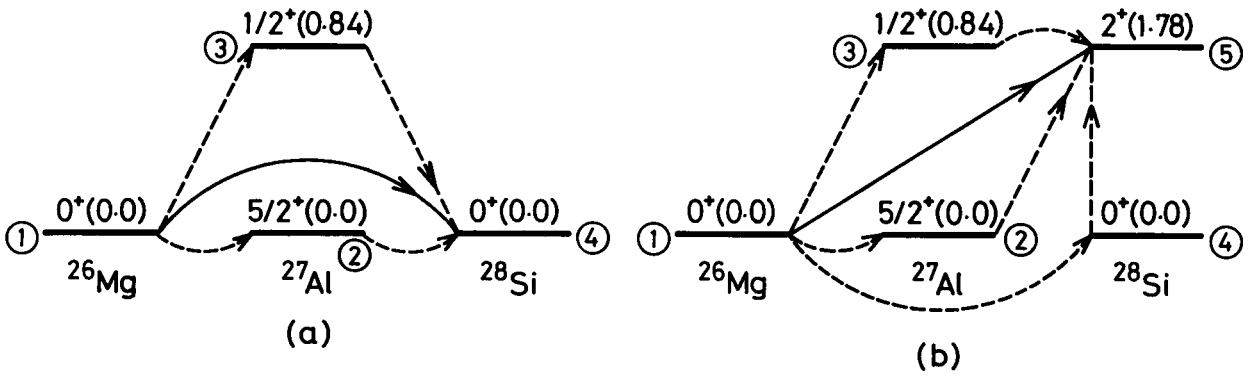

Fig. 1. Channels taken into account in the coupled-channel calculations for the transitions to the ground and the first-excited states in ^{28}Si.

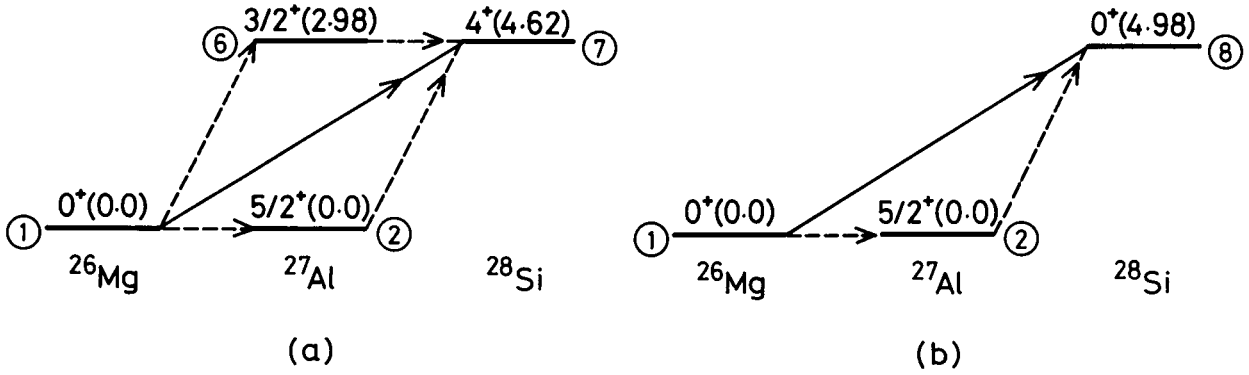

Fig. 2. Channels taken into account in the coupled-channel calculations for the transitions to the second- and the third-excited states in ^{28}Si.

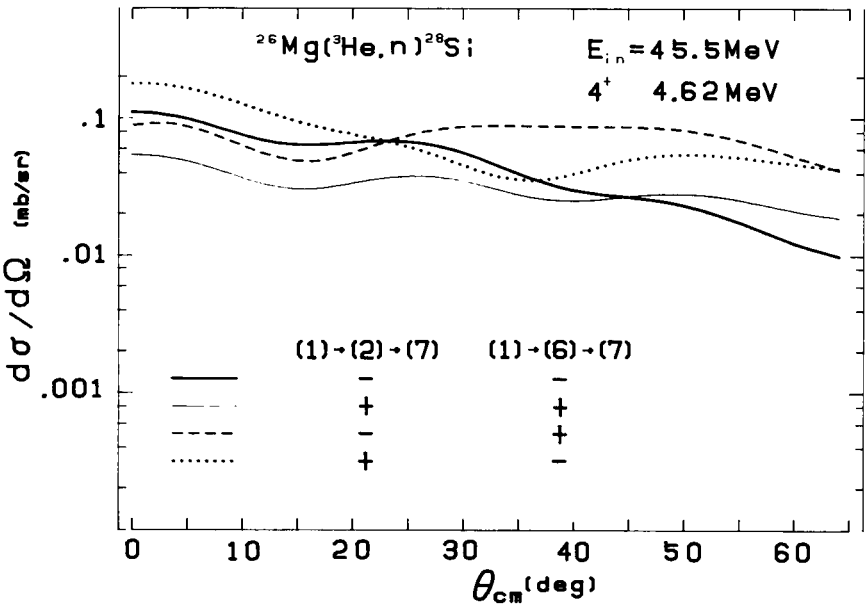

Fig. 3. Results of the coupled-channel calculations for the $^{26}Mg(^{3}He,n)^{28}Si$ reaction leading to the 4.62-MeV 4^{+} state at 45.5 MeV bombarding energy made by assuming four different phase combinations of spectroscopic amplitudes. As for the numbers designating channels, see fig. 2. The shell-model two-nucleon spectroscopic amplitude is used for the direct transition, (1)→(7).

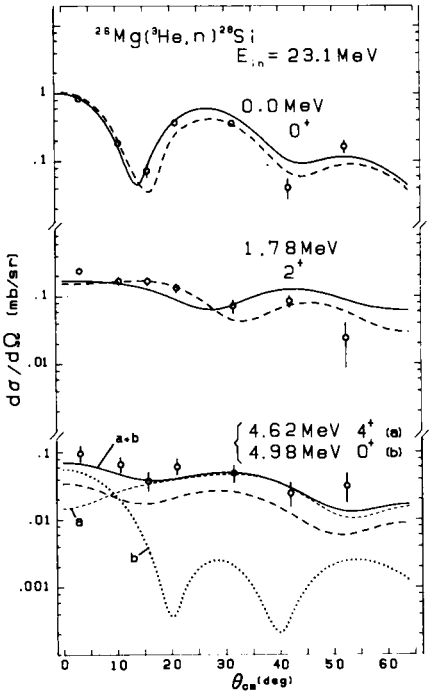

Fig. 4. Neutron angular distributions for the $^{26}Mg(^{3}He,n)^{28}Si$ reaction at 23.1 MeV bombarding energy compared with theoretical predictions.

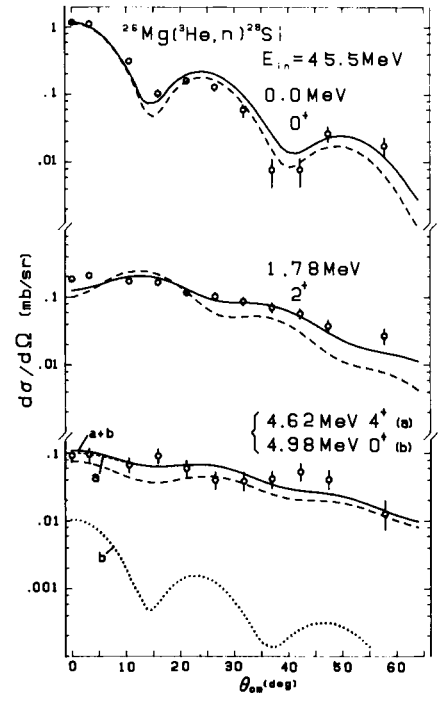

Fig. 5. Neutron angular distributions for the $^{26}Mg(^{3}He,n)^{28}Si$ reaction at 45.5 MeV bombarding energy compared with theoretical predictions.